

POTENTIAL TSUNAMI HAZARD RELATED TO THE SEISMIC ACTIVITY EAST OF
MAYOTTE ISLAND, COMOROS ARCHIPELAGO

Jean Roger^{1,*}

1. LEGOS, Institut de Recherche pour le Développement, 101, Promenade Roger Laroque, BP A5 98848 Nouméa Cedex (contact: jeanrog@hotmail.fr) (Received May 28, 2019, Accepted for publication June 4, 2019)

ABSTRACT

On May 13, 2018, a seismic swarm began to occur east of Mayotte Island, Comoros Archipelago. Only two days after, a strong Mw 5.9 earthquake shook the island and awakened the fears of local people to be struck by a tsunami, in the aftermath of the catastrophic 2004 Indian Ocean event. This paper does not claim to represent a detailed tsunami hazard study, but tries to provide keys about the potential of tsunami generation in the area, explaining point by point the capacity of each source, earthquake, submarine volcanic eruption and landslide to produce perturbation of the sea. Numerical modelling of landslide is presented herein to discuss the relative immunity offered by the coral barrier reef to the island populated coastline to moderate scenarios

1. GENERAL SETTINGS

1a. *Geology*

Mayotte '*Maore*' is a little French island of 374 km² belonging to the Comoros Archipelago, *the islands of the Moon*, at the northern outskirts of the Mozambique Channel, separating Madagascar from Africa (**Fig. 1a**). This archipelago is the surface geological result of a volcanic hotspot beginning to build volcanoes between 15 and 10 million years ago, with an emerged part about 8 to 10 million years ago (**Debeuf, 2009**). Some authors propose a combined tectonic activity on transform faults reactivated by a lithospheric deformation (**Nougier et al., 1986; Michon, 2016**). Mayotte is a volcanic structure rising at least 4400 m above the sea floor (**Audru et al., 2006**), showing a maximum altitude of 660 m a.s.l. only at Mount Bénara (Fig. 1b).

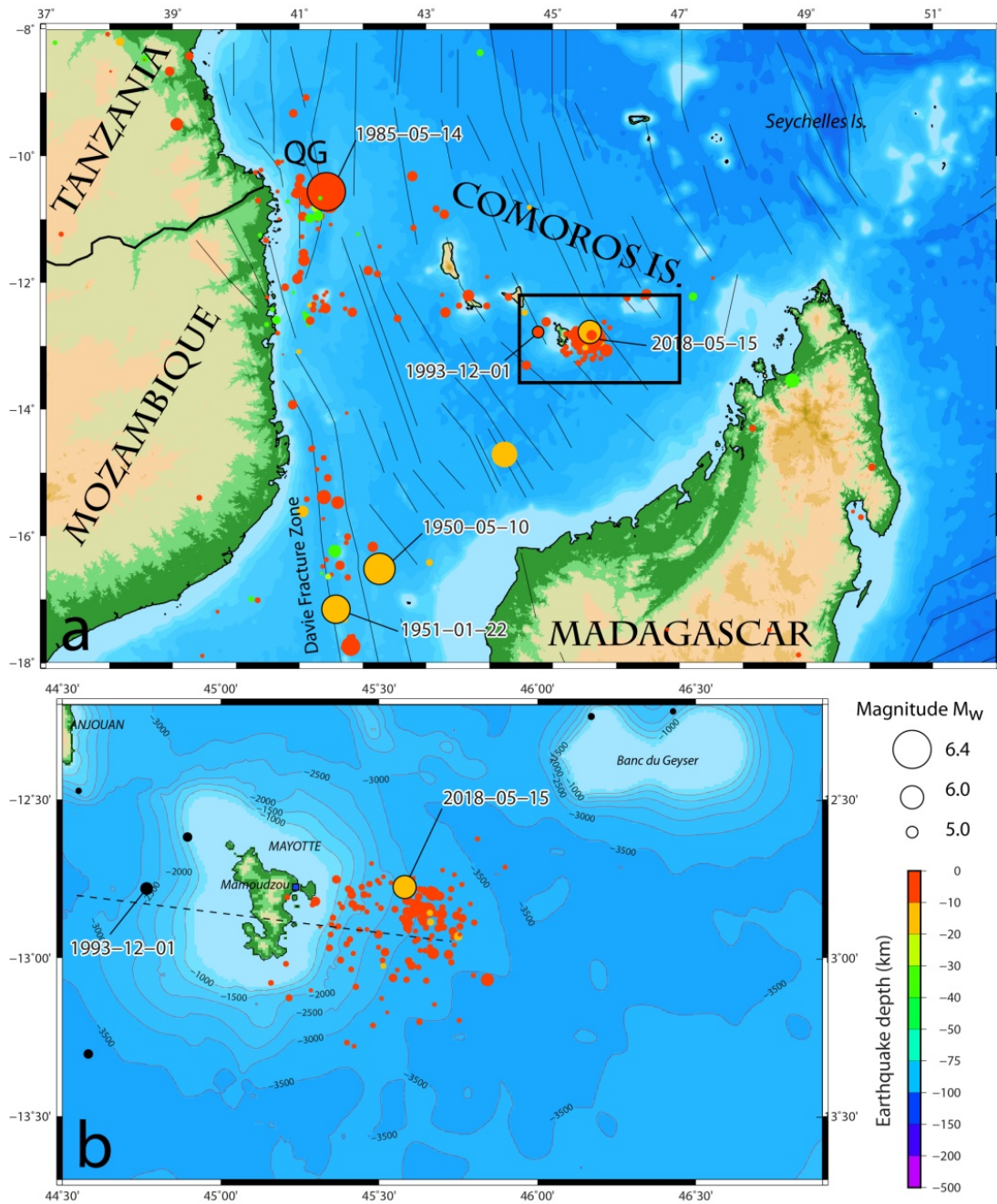


Figure 1: Geologic settings. a) Mayotte is an island of the Comoros Archipelago located within the Mozambique Channel between Madagascar and Mozambique; earthquake epicenters recorded by the USGS since 1950 are shown by colored circles, the size of which is a function of earthquake magnitude; black segments: fractures identified by Phethean et al. (2016). b) Focus on the earthquake swarm since May 15, 2018; black dots: seismic activity before May 15, 2018; black dashed line: profile location shown on figure 2.

The volcanic activity moved progressively toward the North-West, and is now located in Grande Comore. It resulted in the stop of the island growth, which, coupled to an active tropical erosion due to heavy rainfall, led to its subsidence and the slow construction of a coral reef around Mayotte. The lagoon surface is estimated to ~1500 km² lagoon, being among the largest in the world.

1b. Population and natural hazards

Mayotte is a highly populated island relative to its available living surface: in 2017, the population density was estimated to 690 people per square kilometer, rising at a rate of 3.8 % per year (**Genay and Merceron, 2017**).

Until May 2018, amongst the natural hazards commonly affecting Mayotte like heavy rains, storms or landslides, was not the ground shaking or earthquake : in fact, **Audru et al. (2010)** indicate that the French SisFrance earthquake catalog reports only 3 events in 1936, 1941 and 1953 to add to the USGS database, which itself shows only two other recorded events: the Mw 5.2 December 1, 1993 and the Mw 5.0 September 9, 2011 earthquakes. Thus, the island population is not historically prepared for earthquakes as it is the case in very active regions like subduction zones.

1c. The earthquake swarm

On May 13, 2018, a magnitude Mw 4.6 earthquake was widely felt by the island population. It was the first noticeable event of the ongoing earthquake swarm beginning on May 10, 2018 according to instrumental records. It was soon followed, two days later on May 15, 2018, by a stronger Mw 5.9 earthquake. This earthquake did not cause any severe damages and did not cause any severe injuries (only 3 wounded people were reported by local authorities) but caused the whole population to feel concerned by this natural phenomenon. A range of hypotheses have been raised, and amongst them, the possibility of this swarm to be triggered by submarine volcanic activity. This hypothesis is about to be validated by the recent MAYOBS bathymetric survey from a French consortium of research laboratories. The problem in this area is that the geology and tectonics are not very well constrained, and the lack of geophysical data (and especially seismic data) from local stations generates uncertainties concerning the swarm interpretation.

As a result, the population is afraid of what could happen in the near future and lots of people wonder if such an earthquake could be able to trigger a tsunami toward the island coasts, remembering the 2004 Indian Ocean catastrophic event.

1d. Historical tsunamis

Mayotte is not an island known to have been affected severely by tsunamis over the past centuries, but this could simply be a consequence of insufficient written archives. Thus, two events have been reported there recently the November 27, 1945 Makran (Iran) tsunami and the December 26, 2004 Sumatra ocean-wide tsunami (**Lambert and Terrier, 2011**). The first one shows a run-up of 4.05 m in Mayotte and more than 6 m in the neighboring island of Grande Comore (**Okal et al., 2009**). The second one affected the northwestern part of the Indian Ocean, as for example the Seychelles Islands where it has been reported to 30-50 cm (**Heidarzadeh and Satake, 2014**). For information, it also reached about 1 m at Mtsanga Safari

beach on Chissoua Mtsamboro, north of Mayotte (**Matthias Deuss, pers. comm., 2019**) although **Lavigne et al. (2012)** indicate there is no real evidence on Mayotte coastline. Nevertheless, the 2004 event, and all the catastrophic tsunamis that occurred thereafter, have severely impressed the world's population, especially those who are living in coastal areas. Such is the case in Mayotte, where the coastal population is rising wildly (**Bernardie-Tahir and El-Mahaboubi, 2001**): people are now very concerned by natural hazards, amid fears of the ability of the earthquakes to trigger destructive tsunami waves.

2. DIFFERENT ORIGINS

2a. "Earthquake tsunami"

On March 21, 2019, the earthquake swarm was composed of 16 earthquakes of magnitude $M_w \geq 5$ and 161 with $4.0 \leq M_w < 5.0$ according to the USGS database (**U.S. Geological Survey, 2019**). Global tsunami databases such as the NOAA NGDC/WDS tsunami catalogue (www.ngdc.noaa.gov/hazard/tsu_db.shtml) or the Historical Tsunami Database for the World Ocean -HTDB/WLD (<http://tsun.ssec.ru/tsunami-database/index.php>) allow to empirically show that there are no recorded tsunamis triggered by earthquakes of magnitude $M_w < 6.3$ (**Tinti, 1991**). Given that the biggest earthquake of the Mayotte swarm reached only a moment magnitude $M_w = 5.9$, it was normally not sufficient to trigger a tsunami. **Bolt et al. (1975)**, for example, have indicated that the maximum run-up for a tsunami generated by a $M_w = 6.5$ earthquake would be no more than 0.5-0.75 m.

In addition, the moment tensors calculated by the Global CMT project (<https://globalcmt.org>) for the major earthquakes of the seismic swarm exhibit strike-slip mechanisms showing sometimes very limited normal or reverse components. Most of the strike-slip events recorded around the World have not been able to trigger tsunamis but **Tanioka and Satake (1996)** have shown that, in cases where the rupture occurs on a steep slope with a horizontal displacement significantly larger than the vertical displacement, horizontal movement -strike-slip faulting- along a fault plane is also able to trigger a tsunami. In addition, **Legg and Borrero (2001)** and **Borrero et al. (2004)** have also shown that tectonic events occurring on strike-slip faults with sinuous traces could trigger tsunamis by the effect of uplift and subsidence along successions of fault bends and releasing bends. In the case of a substantial increase of earthquakes magnitude ($M_w > 6.3-6.5$) in the swarm area, it would be difficult for a strike-slip mechanism to produce such displacement as most of the earthquake epicenters have been located under the abyssal plain, i.e. in an area where no submarine features like grabens or seamounts have been identified (this information could change after the mapping of the discovered volcanic structure by the MAYOBS survey). In addition, the structures identified by Phethean et al. (2016) and shown on figure 1a seem not able to produce magnitudes sufficient to trigger tsunamis but should be clarified with seismic data.

2b. "Volcanic tsunami"

Volcanic eruptions are also able to trigger tsunamis: 123 of the 2640 tsunamis reported in the NOAA NGDC/WDS tsunami catalogue are attributed to volcanic eruptions, i.e. 4.65 % of the reported tsunamis. About 29% are the results of submarine explosions (**Latter, 1981**) but a handful of them are amongst them, the biggest catastrophic tsunamis like the emblematic eruption of the Krakatoa, Indonesia, on August 26,

1883, which was able to trigger a 15 m high wave on both side of the Sunda Strait, reaching 40 m in some places and killing thousands (**Nomanbhoy and Satake, 1995; Pelinovsky et al., 2005**). In addition, the structures identified by Phethean et. al. (2016) and shown on figure 1a seem not able to produce magnitudes sufficient to trigger tsunamis and should be clarified with seismic data.

Another catastrophic event is the Santorini, Greece, explosion circa 1470 BC and having triggered a powerful tsunami with impacts on nearby islands. But most of the time, the tsunamis following volcanic eruptions are triggered not by the explosion itself as in the two previous cases, but because of induced landslides, rock falls or pyroclastic flows. In order to understand the tsunami generation mechanism by underwater explosions only a few studies like the ones by **Duffy (1992)** and **Egorov (2007)** have been conducted over the past decades, probably because tide gauge data for such tsunamis are seriously lacking (**Belousov et al., 2000**). Nevertheless, in case an underwater explosion occurs it has been shown that the generation of a tsunami is directly linked to thresholds of heterogeneous and homogeneous hydroexplosion related to water depths of respectively 675 m and 130 m (**Smith and Shepherd, 1993**). Considering this study, in the specific case of Mayotte, if the submarine volcanic structure identified by the MAYOBS survey in the swarm area turns out to be linked to the earthquakes, it corresponds to a ~800 m high edifice lying on depths of ~2500-3000 m, and thus, it is unlikely for such a scenario to occur. But as detailed by **Paris (2015)**, all submarine eruptions show different behavior and the depth of the volcano is not the only parameter to consider in the equation. For example, the author indicates that the caldera collapse duration could also be an important factor to deal with.

2c. "Landslide tsunami"

Landslides are relatively frequent events occurring at active continental margins or on the slopes of oceanic islands, especially if these islands are located into areas of plate convergence. Tsunamis generated by landslides are quite common and these landslides could be associated with other natural hazards like heavy rainfall, earthquakes or volcanic eruptions. Tsunamis triggered by landslides show the most impressive amplitudes and run-up heights, especially events like the 1958 tsunami in Lituya Bay, Alaska, which attained a maximum run-up limit of 524 m above mean sea level (**Gonzalez-Vida et al., 2019**). But although they could show high amplitudes near the source, they are also prone to important energy dispersion phenomenon. It is important to note that a large number of massive landslide-triggered tsunamis have been caused by earthquakes like the 1929 Grand Bank, Newfoundland or the more recent December 2018 Anak Krakatau, Indonesia events.

In the present case study, it is worth noting that landslides would occur mainly on the slopes of Mayotte Island itself. The BATHYMAY survey (**Audru et al., 2006**) has highlighted the presence of steep slope angles in excess of 15° (as shown on **figure 2**) and numerous submarine canyons, in addition to well identified faults network, sometimes striking through the barrier reef. It is thus easy to imagine that the multitude of earthquakes of the swarm probably affected the stability of these slopes, especially the earthquakes located closest to the island (westernmost events) and showing the strongest intensities.

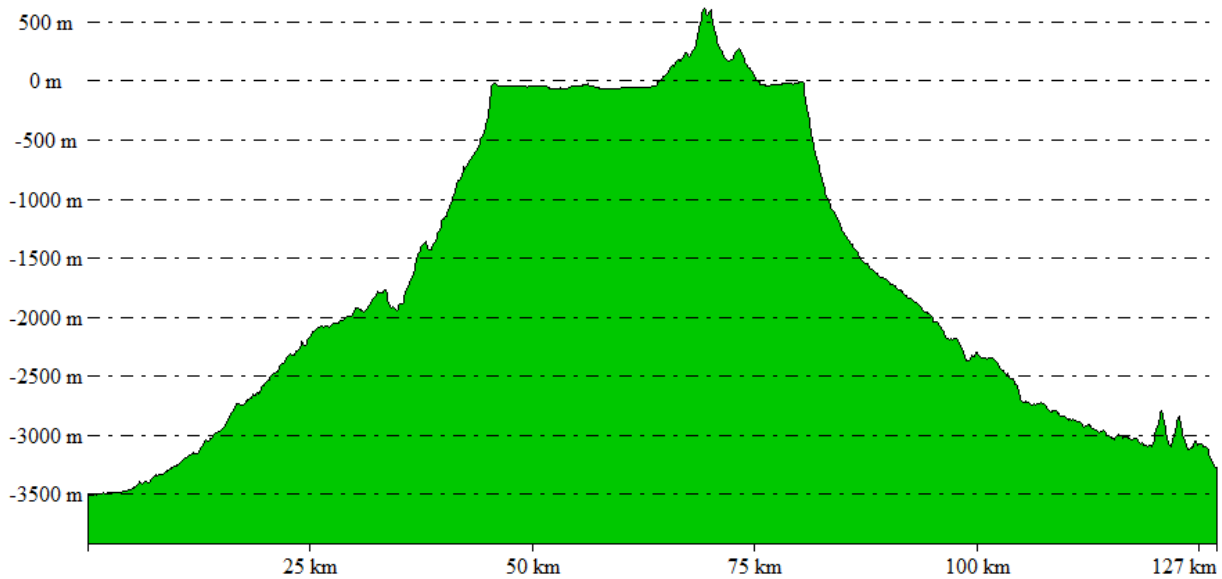


Figure 2: Cross profile of Mayotte D.E.M. (associated to SRTM topographic data) showing steep slopes. The profile location is indicated in figure 1. Bathymetric data are from the SHOM (2016) and Topographic data above sea level are SRTM 3 arcseconds data.

In case a landslide occurred very close to the island, it would be important to determine in what proportion the barrier reef (if not part of the landslide) and lagoon width would play a protective role, attenuating the wave energy by way of energy dispersion and friction occurring at the lagoon floor.

3. NUMERICAL MODELING

Tsunami modeling is used to estimate the role played by the coral reef and the lagoon surrounding Mayotte Island during the tsunami propagation. The objective is not to propose a set of scenarios to produce hazard maps but to discuss the capacity of a tsunami triggered by a submarine landslide to impact Mayotte coastline. For this purpose, only two different cases of relevant submarine landslide scenarios are detailed.

3a. GEOWAVE

The modelings was carried out using GEOWAVE software. This is a package consisting of two different modules: the TOPICS module, which computes the initial deformation of the sea floor with different options of slope mass movements (debris flow, rotational slump, etc.); and the FUNWAVE module, in which this initial deformation is introduced as an input for computing the tsunami propagation and inundation if needed (Watts et al., 2003). The robustness and accuracy of GEOWAVE have been validated through numerous studies all around the world (e.g. Watts et al., 2003; Ioualalen et al., 2006; Grilli et al., 2007; Watts and Tappin, 2012). In the specific case of landslide modeling, it is interesting to indicate that the model uses a finite element scheme to solve the non-linear Boussinesq equations and considers dispersion behavior.

3b. Digital Elevation Model

As an input to the model, a digital elevation model (D.E.M.) showing a resolution of ~180 m was prepared by degrading the available 0.001° resolution D.E.M. from the SHOM (French Navy Oceanographic and Hydrographic Office; **SHOM, 2016**), and was combined with SRTM 3 arcseconds data (~90m at the equator; **Jarvis et al., 2008**) for land topography. This resolution was chosen to answer both to the software calculation limitations and to reproduce the underwater features and the coral barrier surrounding the island as well as possible. The resulting D.E.M. is presented on figure 3.

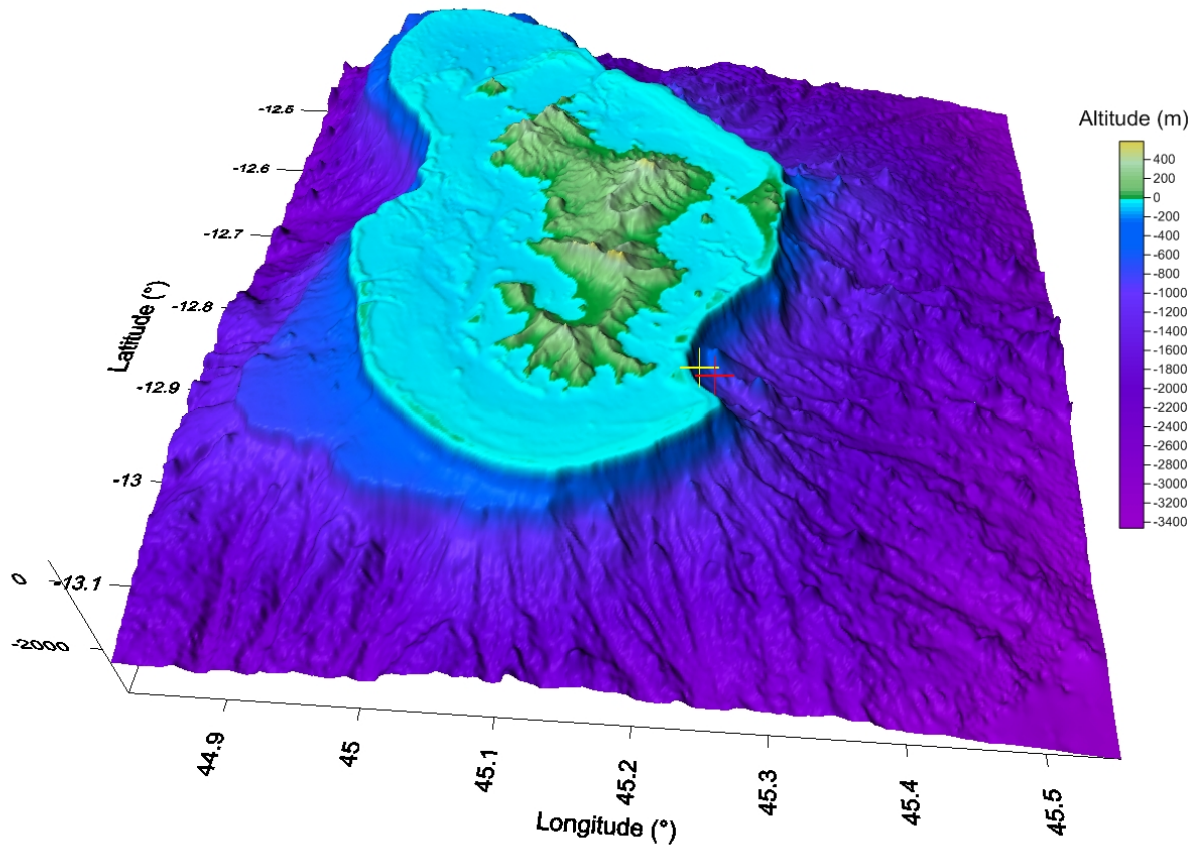


Figure 3 : 180 m resolution digital elevation model (D.E.M.) of Mayotte Island prepared with bathymetric data from the SHOM and SRTM topographic data. Yellow and red crosses locate respectively V1 and V2 landslide gravity centroids used in the modeling.

3c. Scenarios

It is important to consider the local geology before modeling underwater landslides. The numerical modeling software needs some source parameters to compute the initial deformation surface. In this case, it has been decided to consider rotational slump behavior in agreement with available literature about landslides on volcanic islands (e.g. **Whelan and Kelleat, 2003**).

The most important parameter of a landslide for triggering a tsunami is its initial velocity (**Lovholt et al., 2015**), which itself is directly linked to the volume and density of the moving material and to slope angle. The volume depends on the characteristic length L , width W and thickness T of the sliding material. The ratios between these parameters are consistent with previous studies (e.g. **Yamagishi and Ito, 1994**).

According to the fact that Mayotte is a volcanic island surrounded by a well-developed calcareous reef, the bulk density of the sliding of potentially unconsolidated material has been arbitrarily chosen as 2000 kg/m^3 , a plausibly low value of water-saturated sandstone bulk density (**Manger, 1963**). Run-out distances have been chosen to stay within the stability window of GEOWAVE.

We chose to model two landslide scenarios located on the south-east flank of the island (yellow and red crosses in **Figure 3**) in a region where the shape of the bathymetry could be associated to one or several submarine landslides. The parameters of the two landslides are given in **Table 1**.

The volumes have been chosen in agreement with available literature about submarine landslides and correspond to "classical" medium-size slope-failure events of respectively 0.012 and 0.12 km^3 .

Scenario	V1	V2
V (km ³)	0.012	0.12
x_0 (°)	45.24°E	45.25°E
y_0 (°)	-12.97	-12.97
d (m)	560	800
L (m)	600	1500
W (m)	400	400
T (m)	50	200
Φ (°)	270	270
Θ (°)	16	16
MWH(m)	0.69	3.21

Table 1: Parameters for the two rotational slump scenarii as introduced in GEOWAVE. V corresponds to the landslide volume, x_0 , y_0 and d to the longitude, latitude and depth of the center of mass, L , W and T to the length, width and thickness of the volume, Φ to the azimuth and Θ to the slope angle. MWH represents the maximum value of the sea level reached at one node of the grid.

4. RESULTS

The two scenarios have been modeled with GEOWAVE for a propagation time of 30 minutes over the 180 m resolution D.E.M.

Figure 4 shows numerical propagation of the tsunami triggered by scenario V2. It highlights the propagation of a ~3 m high tsunami (maximum value = 3.21 m) in an isotropic way (except for the lagoon part, in the west) from the first seconds to 28 minutes of the model run. At the very first time of the propagation (= first minute), the shape of the tsunami is directly related to the landslide parameters including the runout length. In the present case it shows a "flying bird" shape produced by the moving material toward the east that will evolve quickly to an alternating pattern of peaks and troughs radiating from the source region.

It shows clearly that after less than 30 minutes, and due to wave dispersion and wrapping around the barrier reef, the energy loss leads to tsunami disappearance (amplitude goes from 3 m to less than 5 cm).

The wave train entering the lagoon reaches the coastline in less than 10 minutes, travel time directly linked to the lagoon width and depth in front of the source location.

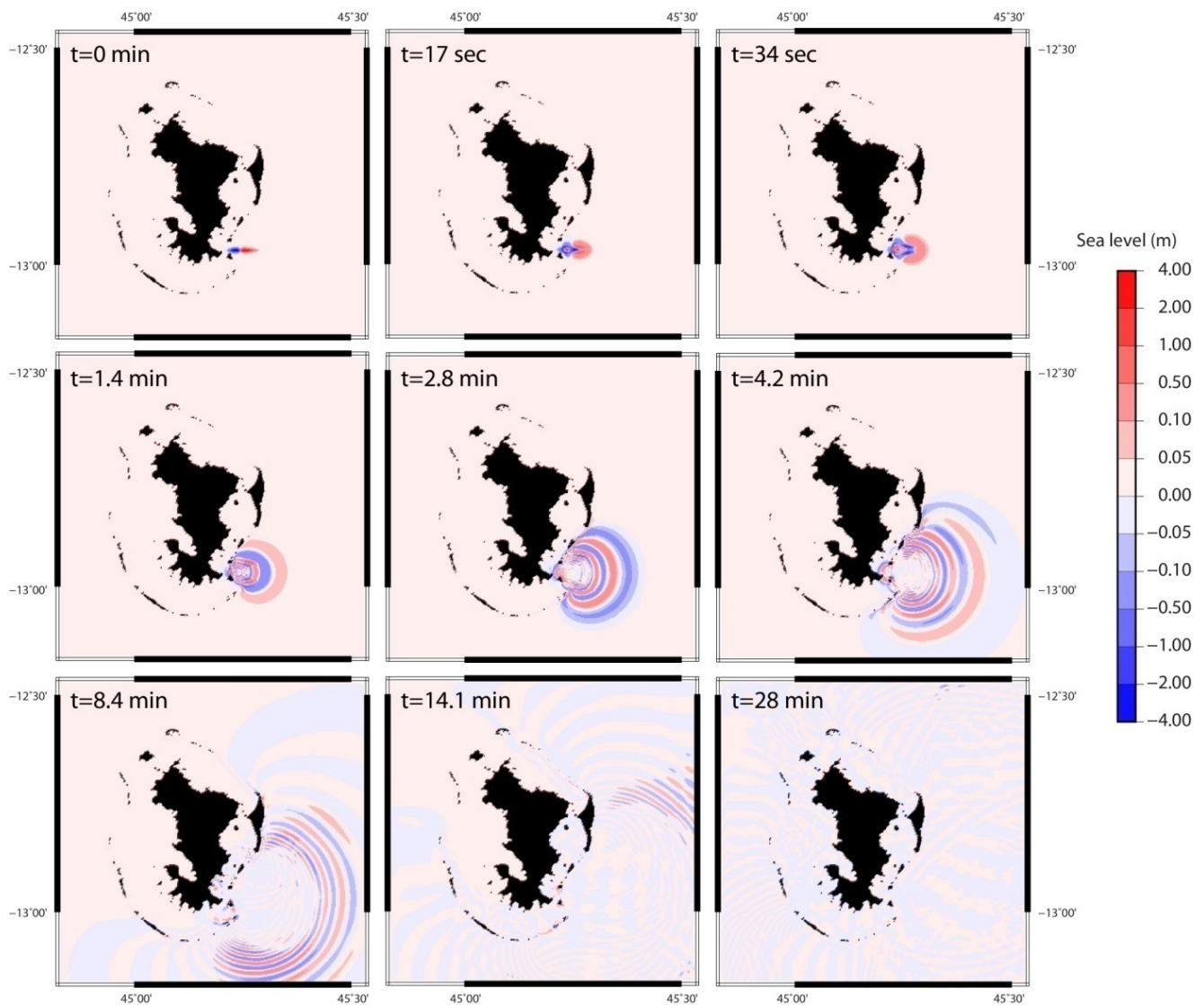


Figure 4 : Propagation of a tsunami triggered by a landslide on Mayotte Island southeastern slope.

Figure 5 presents the maximum wave heights maps for scenarii V1 and V2 representing the maximum wave height reached on each nodes of the grid during the whole propagation. As during the propagation process, the "flying bird" shape is also associated to the maximum wave heights recorded on the whole grid with value ranging between 0.4 and 1 m for scenario V1 and between 1 and 3.2 m for scenario V2. In both cases, the high values shown on the west of the source, close to the barrier reef, correspond to wave shoaling when the water depth decreases on the island slope.

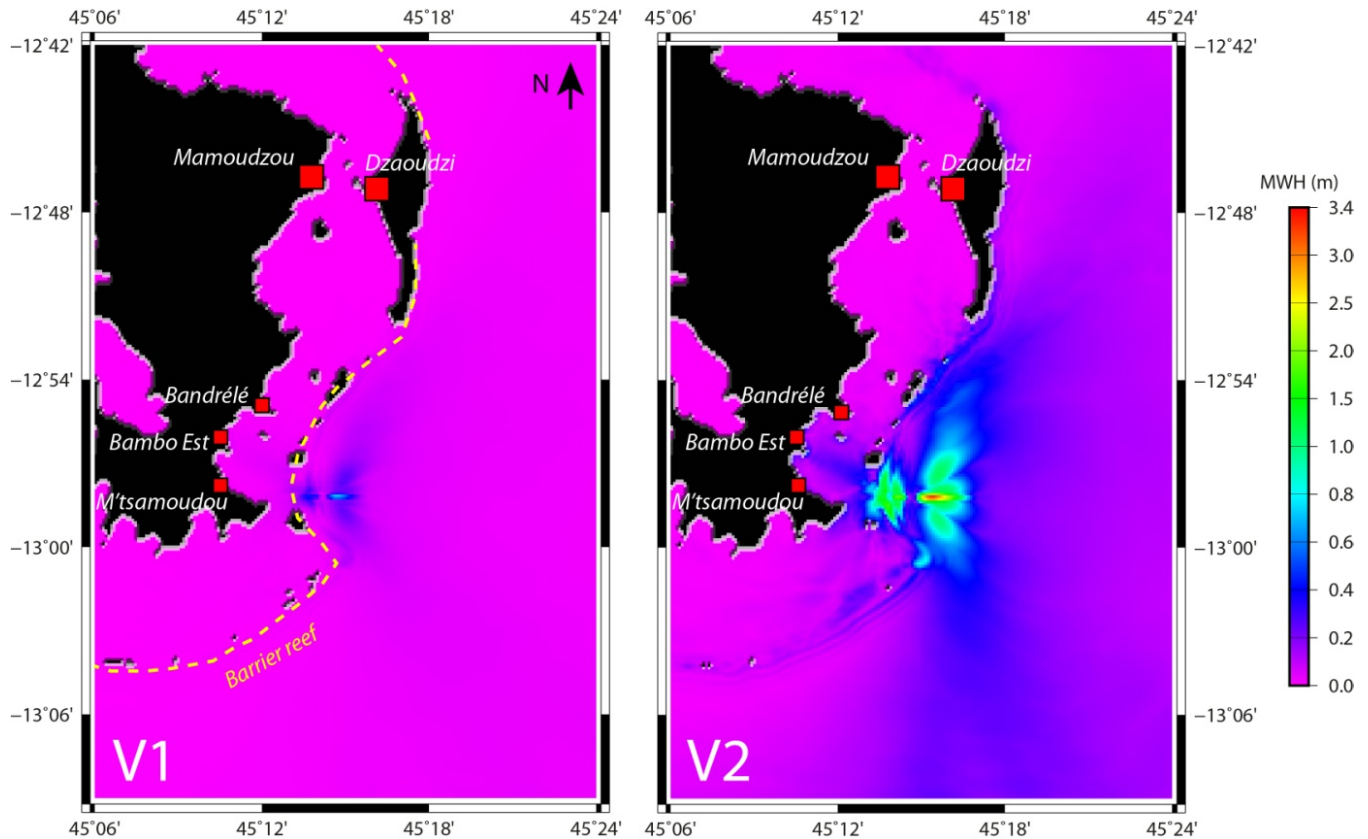


Figure 5: Focus on the maximum wave height maps (MWH) for V1 and V2 scenarii in the source area after 33 min of tsunami propagation. Some towns and villages are symbolized with red squares. Yellow dashed line: coral barrier reef.

Except the difference of wave heights and dispersion between the two scenarios, it reveals that in such cases:

- the barrier reef plays a protective role against tsunami waves triggered by landslides (showing high frequency waves in comparison to tsunamis triggered by earthquakes): in the case of scenario V1, there is no significant sea level change inside the lagoon and for scenario V2, the maximum height is divided by at least 6 from 3.2 m (maximum value) to 0.5 m maximum inside the lagoon;
- the maximum wave heights do not exceed 0.5 m at a distance of circa 10 km away from the source (scenario V2).

5. CONCLUSIONS

This study indicates that the actual knowledge of the geology in Mayotte region, including the recent discovery of a submarine volcano within the seismic swarm area east of the island, enable to conclude that neither an earthquake within the actual magnitude range ($M_w < 6.0$), nor a volcanic eruption (at the actual volcano summit depth) could trigger a tsunami having an impact onto the island's coast. However, the numerous earthquakes which seem to be related to the volcanic activity could produce submarine landslides along Mayotte slopes, which landslides are potentially able to trigger tsunamis.

Currently, it is not known whether the seismic swarm has been already able to trigger such landslides, even small, along Mayotte. Only small landslides have been identified on land, but those could also be related to frequent heavy rainfalls.

In order to give keys to assess landslide generated tsunami hazard, two landslide scenarii have been modeled. The results of tsunami modeling presented hereabove show that the tsunami shape and coastal impact are directly linked to the volume of the landslide as already demonstrated by numerous studies in other regions. They also highlight the role played by the coral barrier reef in terms of mitigation of the tsunami hazard, and this information should be considered by decision-makers to protect these valuable ecosystem surrounding Mayotte.

It is important to notice that the two modeled scenarii are based on available literature on submarine landslides and not on geological facts reported around Mayotte. The objective was only to estimate what could happen in case an earthquake destabilizes unconsolidated sediments or a part of the barrier reef. To make an accurate hazard study about tsunamis triggered by landslides, the first most important thing would be to identify all scars of past landslides that could exist along the island margin and estimate the mobilized volumes. The second step would be to identify and map the potential unstable areas, if they exist, and to propose realistic volumes for each one. These values could then be entered as data in further model runs. In addition, the tide level should also be considered as Mayotte is subject to a maximum tidal range of ~4 m, modeling the same tsunamis at low and high tides.

ACKNOWLEDGMENTS

The author is very grateful to Yanni Gunnell who kindly proofread the manuscript.

Funding

This study has not been funded.

REFERENCES

- Audru, J.-C., Bitri, A., Desprats, J.-F., Dominique, P., Eucher, G., Hachim, S., Jossot, O., Mathon, C., Nédellec, J.-L., Sabourault, P., Sedan, O., Stollsteiner, P., Terroer-Sedan, M. (2010).** Major natural hazards in a tropical volcanic island: A review for Mayotte Island, Comoros archipelago, Indian Ocean. *Engineering Geology*, 114, 364-381.
- Audru, J.-C., Guennoc, P., Thinon, I., Abellard, O. (2006).** BATHYMAY: underwater structure of Mayotte Island revealed by multibeam bathymetry. *Comptes-Rendus Geosciences*, 338(16), 1240-1249.
- Belousov, A., Voight, B., Belousova, M., Muravyev, Y. (2000).** Tsunamis generated by subaquatic volcanic explosions: unique data from 1996 eruption in Karymskoye Lake, Kamchatka, Russia. *Pure and Applied Geophysics*, 157, 1135-1143.
- Bernardie-Tahir, N., El-Mahaboubi, O. (2001).** Mayotte: des parfums au tourisme. Les nouveaux enjeux du littoral. *Les Cahiers d'Outre-Mer*, 216, 369-396.
- Bolt, B.A., Horn, W.L., Macdonald, G.A., Scott, R.F. (1975).** Geological Hazards. Earthquakes - Tsunamis - Volcanoes - Avalanches - Landslides - Floods. Springer-Verlag, 329 pp., 116 fig., doi : 10.1007/978-3-642-86820-7.
- Borrero, J.C., Legg, M.R., Synolakis, C.E. (2004).** Tsunami sources in the southern California bight. *Geophysical Research Letters*, 31(13), L13211, doi : 10.1029/2004GL020078.
- Debeuf, D. (2009).** Etude de l'évolution volcano-structurale et magmatique de Mayotte, archipel des Comores, océan Indien: approche structurale, pétrographique, géochimique et géochronologique. Thèse de volcanologie, Université de la Réunion, 277 pp.
- Duffy, D.G. (1992).** On the generation of oceanic surface waves by underwater volcanic explosions. *Journal of Volcanology and Geothermal Research*, 50(3), 323-344, [https://doi.org/10.1016/0377-0273\(92\)90100-R](https://doi.org/10.1016/0377-0273(92)90100-R).
- Egorov, Y. (2007).** Tsunami wave generation by the eruption of underwater volcano. *Natural Hazards and Earth System Sciences*, 7, 65-69.
- Genay, V., Merceron, S. (2017).** 256500 habitants à Mayotte en 2017. *INSEE FOCUS*, 105, <https://www.insee.fr/fr/statistiques/3286558>.
- Gonzalez-Vida, J., Macias, J., Castro, M.J., Sanchez-Linares, C., de la Asuncion, M., Ortega-Acosta, S., Arcas, D. (2019).** The Lituya Bay landslide-generated mega-tsunami - numerical simulation and sensitivity analysis. *Natural Hazards and Earth System Sciences*, 19, 369-388.
- Grilli, S.T., Ioualalen, M., Asavanant, J., Shi, F., Kirby, J.T., Watts, P. (2007).** Source constraints and model simulation of the December 26, 2004 Indian Ocean tsunami. *Journal of Waterways, Port, Coastal and Ocean Engineering*, 133(6), [https://doi.org/10.1061/\(ASCE\)0733-950X\(2007\)133:6\(414\)](https://doi.org/10.1061/(ASCE)0733-950X(2007)133:6(414)).

- Heidarzadeh, M., Satake, K. (2014).** New insights into the source of the Makran tsunami of 27 November 1945 from tsunami waveforms and coastal deformation data. *Pure and Applied Geophysics*, 172(3-4), 621-640, <https://doi.org/10.1007/s00024-014-0948-y>.
- Ioualalen, M., Pelletier, B., Watts, P., Regnier, M. (2006).** Numerical modeling of the 26th November 1999 Vanuatu tsunami. *Journal of Geophysical Research*, 111, C06030, <https://doi.org/10.1029/2005JC003249>.
- Ioualalen, M., Asavanant, J., Kaewbanjak, N., Grilli, S.T., Kirby, J.T., Watts, P. (2007).** Modeling the 26 December 2004 Indian Ocean tsunami: Case study of impact in Thailand. *Journal of Geophysical Research*, 112, C07024, <https://doi.org/10.1029/2006JC003850>.
- Jarvis, A., Reuter, H.I., Nelson, A., Guevara, E. (2008).** Hole-filled SRTM for the globe Version 4, available from the CGIAR-CSI SRTM 90M Database (<http://srtm.csi.cgiar.org>).
- Lambert, J., Terrier, M. (2011).** Historical tsunami database for France and its overseas territories. *natural Hazards and Earth System Sciences*, 11, 1037-1046.
- Latter, J.H. (1981).** Tsunamis of volcanic origin: Summary of causes, with particular reference to Krakatoa, 1883. *Bulletin of Volcanology*, 44(3), 467-490.
- Lavigne, F., Sahal, A., Coquet, M., Wassmer, P., Goett, H., Leone, F., Péroche, M., Lagahé, E., Gherardi, M., Vinet, F., Hachim, S., Drouet, F., Quentel, E., Loevenbruck, A., Schindelé, F., Hébert, H., Anselme, B., Durand, P., Gaultier-Gaillard, S., Pratlong, F., Divialle, F., Morin, J. (2012).** PREPARTOI. Final Report, 257 pp.
- Legg, M.R., Borrero, J.C. (2001).** Tsunami potential of major restraining bends along submarine strike-slip faults. *ITS 2001 Proceedings*, session 1, Number 1-9, 331-342.
- LØvholt, F., Pedersen, G., Harbitz, C.B., Glimsdal, S., Kim, J. (2015).** On the characteristics of landslide tsunamis. *Philosophical Transactions A, Math. Phys. Eng. Sci.*, 373(2053), 20140376, <https://doi.org/10.1098/rsta.2014.0376>.
- Nomanbhoy, N., Satake, K. (1995).** Generation mechanism of tsunamis from the 1883 Krakatau eruption. *Geophysical Research Letters*, 22(4), 509-512.
- Nougier, J., Cantagrel, J.M., Karche, J.P. (1986).** The Comores archipelago in the western Indian Ocean: volcanology, geochronology and geodynamic setting. *Journal of African Earth Sciences*, 5(2), 135-145.
- Manger, G.E. (1963).** Porosity and bulk density of sedimentary rocks. *Contributions to geochemistry. Geological Survey Bulletin*, 1144-E
- Michon, L. (2016).** The volcanism of the Comoros archipelago integrated at a regional scale. In: Bachelery, P., Lénat, J.-F., Di Muro, A. and Michon, L. (Eds.), *Active Volcanoes of the Southwest Indian Ocean: Piton de la Fournaise and Karthala*, Springer-Verlag, 233-244, *Active Volcanoes in the World*, 978-3-642-31394-3.

- Okal, E.A., Fritz, H.M., Sladen, A. (2009).** 2004 Sumatra-Andaman tsunami surveys in the Comoro Islands and Tanzania and regional tsunami hazard from future Sumatra events. *South African Journal of Geology*, 112, 343-358.
- Paris, R. (2015).** Source mechanisms of volcanic tsunamis. *Philosophical Transactions of the Royal Society A*, 373, 20140380, <http://dx.doi.org/10.1098/rsta.2014.0380>.
- Pelinovsky, E., Choi, B.H., Stromkov, A., Didenkulova, I., Kim, H.-S. (2005).** Analysis of tide-gauge records of the 1883 Krakatau tsunami. In: Satake, K. (eds): *Tsunamis. Advances in Natural and Technological Hazards Research*, Springer, 23, 57-77.
- Phethean, J.J.J., Kalnins, L.M., van Hunen, J., Biffi, P.G., Davies, R.J., McCaffrey, K.J.W. (2016).** Madagascar's escape from Africa: A high-resolution plate reconstruction for the Western Somali Basin and implications for supercontinental dispersal. *Geochemistry, Geophysics, Geosystems*, 17(12), 5036-5055, <https://doi.org/10.1002/2016GC006624>.
- SHOM (2016).** MNT bathymétrie de la façade de Mayotte (Projet Homonim). http://dx.doi.org/10.17183/MNT_MAY100m_HOMONIM8WGS84.
- Smith, M.S., Shepherd, J.B. (1993).** Preliminary investigations of the tsunami hazard of Kick'em Jenny submarine volcano. *Natural Hazards*, 7, 257-277.
- Tanioka, Y., Satake, K. (1996).** Tsunami generation by horizontal displacement of ocean bottom. *Geophysical Research Letters*, 23(8), 861-864.
- Tinti, S. (1991).** Evaluation of tsunami hazard in Calabria and Eastern Sicily, Italy. In: *Tsunamis in the World* (Ed.: S. Tinti), 141-157.
- U.S. Geological Survey (2019).** Earthquake catalogue: accessed March 21, 2019 at URL <https://earthquake.usgs.gov/earthquakes/search/>.
- Watts, P., Grilli, S.T., Kirby, J.T., Fryer, G.J., Tappin, D.R. (2003).** Landslide tsunami case studies using a Boussinesq model and a fully nonlinear tsunami generation model. *Natural Hazards and Earth System Sciences*, 3(5), 391-402.
- Watts, P., Tappin, D.R. (2012).** Geowave validation with case studies: Accurate geology reproduces observations. In: Yamada Y. et al. (eds) *Submarine Mass Movements and Their Consequences. Advances in Natural and Technological Hazards Research*, 31, 517-524, https://doi.org/10.1007/978-94-007-2162-3_46.
- Whelan, F., Kelletat, D. (2003).** Submarine slides on volcanic islands - a source for mega-tsunamis in the quaternary. *Progress in Physical Geography*, 27(2), 198-216.
- Yamagishi, H., Ito, Y. (1994).** Relationship of the landslide distribution to geology in Hokkaido, Japan. *Engineering Geology*, 38(3-4), 189-203, [https://doi.org/10.1016/0013-7952\(94\)90037-X](https://doi.org/10.1016/0013-7952(94)90037-X).